

COMBUSTION AND HEAT TRANSFER INTERACTION IN A RADIANT POROUS BURNER

Roberto Carlos Moro Filho, rmoro@ita.br

Amilcar Porto Pimenta, amilcar@ita.br

Departamento de Energia - IEME

Instituto Tecnológico de Aeronáutica – ITA

12228-900 – São José dos Campos – SP - Brasil

Abstract. *This paper presents numerical methods for the simulation of combustion processes in porous media using a 1-step global mechanism. The model is based on a macroscopic formulation of the heat and mass transport equations for laminar flow. The effects of the model on temperature, and species are examined.*

Keywords: *porous media burner, premixed flame, numerical simulation.*

1. INTRODUCTION

According to Pantangi et al. (2006), porous media combustion devices can be classified into two categories, one in which the combustion is fully confined within the pores of the porous structure and the other one in which the combustion takes place over the surface of the porous matrix. The first one is receiving more attention of researchers due to the numerous advantages, burning of lean combustible mixtures, higher ranges of flame stability, lower pollutant formation, etc. (Howell et al. (1996)). Systems based on fluidized bed combustion, in-situ combustion for oil recovery, household heating combustion, are just a few examples of such applications (Trimis and Durst (1996)).

In most of the studies of premixed combustion within inert porous media the flow is assumed to be laminar and one-dimensional, the change in the pressure across the flame is generally negligible compared to the absolute pressure, and the pressure is assumed constant (Baek (1989), Yoshizawa et al. (1988), Hsu et al. (1993), Neef et al. (1999)). The use of single-step global chemistry (Mohamad et al. (1994)) is common. The inadequacies of global kinetics are well recognized, Hsu et al. (1993) presents a comparison between one-step and multi-step chemistry.

Studies on macroscopic transport modeling of incompressible flows in porous media have been based on the volume-average methodology for either heat or mass transfer.

Because of important influence of lateral heat loss in porous medium burners, a two dimensional model is necessary. The present paper follows the foregoing works and presents a two dimensional mathematical model for laminar premixed flame combustion in porous media. Although in this work only one-dimensional plots are presented computations of a two-dimensional laminar pre-mixed flame of methane/air were run. The numerical methodology employed is based on the control-volume approach with a boundary-fitted non-orthogonal coordinate system. The reactor consists of a two-region burner with a small pore size upstream and a large pore size downstream in order to achieve steady combustion in the porous media, the flame can be stabilized at the interface between the two different porosity blocks. The effects of thermal power and radiation are discussed. Multi-step, dispersion and thermal nonequilibrium are subjects of ongoing investigations and will be addressed in subsequent papers.

2. MACROSCOPIC TRANSPORT EQUATIONS

2.1 Macroscopic continuity equation

$$\nabla \cdot \mathbf{u}_D = 0 \quad (1)$$

where, \mathbf{u}_D is the average surface velocity (also known as seepage, superficial, filter or Darcy velocity). Equation (1) represents the macroscopic continuity equation for an incompressible fluid.

2.2 Macroscopic momentum equation

$$\rho \left[\nabla \cdot \left(\frac{\mathbf{u}_D \mathbf{u}_D}{\phi} \right) \right] = -\nabla(\phi \langle p \rangle^i) + \mu \nabla^2 \mathbf{u}_D - \left[\frac{\mu \phi}{K} \mathbf{u}_D + \frac{c_F \phi \rho |\mathbf{u}_D| \mathbf{u}_D}{\sqrt{K}} \right] \quad (2)$$

where the last two terms in equation (2), represent the Darcy-Forchheimer contribution. The symbol K is the porous medium permeability, $c_F = 0.55$ is the form drag coefficient (Forchheimer coefficient), $\langle p \rangle^i$ is the intrinsic (volume-averaged on fluid phase) pressure of the fluid, ρ is the fluid density and is a function of temperature, μ represents the fluid dynamic viscosity and ϕ is the porosity of the porous medium.

2.3 Macroscopic Energy Equation

$$(\rho c_p)_f \nabla \cdot (\mathbf{u}_D \langle T \rangle^i) = \nabla \cdot \{ \mathbf{K}_{eff,f} \cdot \nabla \langle T \rangle^i \} + \phi \Delta H S_{fu} \quad (3)$$

where, $\langle T \rangle^i$ is the averaged temperature for both the solid and the liquid according to the concept of local thermal equilibrium Kaviany (1995), ΔH is the heat of combustion, S_{fu} is the rate of fuel consumption determined by a one-step Arrhenius rate equation, to be shown below, \mathbf{K}_{eff} is the effective conductivity tensor given by,

$$\mathbf{K}_{eff} = \left\{ \phi k_f + (1 - \phi) \left[k_s + \frac{16\sigma \langle T \rangle^i{}^3}{3K_r} \right] \right\} \mathbf{I} + \underbrace{\mathbf{K}_{tor}}_{tortuosity} + \underbrace{\mathbf{K}_{disp}}_{dispersion} \quad (4)$$

where, k_f and k_s are the thermal conductivities for the fluid and for the solid, K_r is the local Rosseland mean attenuation coefficient, σ is the Stefan-Boltzmann constant.

2.4 Macroscopic Mass Transport Equation

$$\nabla \cdot (\mathbf{u}_D \langle m_{fu} \rangle^i) = \nabla \cdot \mathbf{D}_{eff} \cdot \nabla (\phi \langle m_{fu} \rangle^i) + \phi S_{fu} \quad (5)$$

where m_{fu} is the local mass fraction for the fuel. The effective dispersion tensor, \mathbf{D}_{eff} , is defined as:

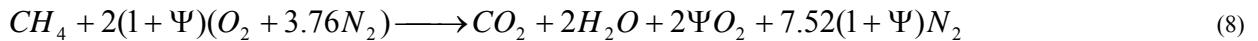
$$\mathbf{D}_{eff} = \mathbf{D}_{disp} + \mathbf{D}_{diff} = \mathbf{D}_{disp} + \frac{1}{\rho} \left(\frac{\mu_\phi}{Sc_\ell} \right) \mathbf{I} \quad (6)$$

where \mathbf{D}_{diff} is the macroscopic diffusion tensor,

$$\mathbf{D}_{diff} = \langle D \rangle^i \mathbf{I} = \frac{1}{\rho} \frac{\mu_\phi}{Sc} \mathbf{I} \quad (7)$$

2.5 Combustion model

Premixed fuel and air enter the system which is characterized by two regions having different porosities. The region at the upstream end has a lower porosity than the one at the downstream end which works as a combustion chamber. The combustion reaction is assumed to occur in a single step according to the chemical equation



where, Ψ is the excess air in the reactant stream at the inlet of porous foam and is related to the equivalent ratio Φ by,

$$\Psi = \frac{1}{\Phi} - 1 \quad (9)$$

where,

$$\Phi = \frac{(m_{fu} / m_{ox})}{(m_{fu} / m_{ox})_{st}} \quad (10)$$

The ratio of fuel consumption is given by,

$$S_{fu} = \rho^2 A \langle m_{fu} \rangle^i \langle m_{ox} \rangle^i \exp[-E_a / R \langle T \rangle^i] \quad (11)$$

where, A is the pre-exponential factor, E_a is the activation energy and R is the universal gas constant. The gas density is updated using the ideal gas equation in the form,

$$\rho = P_0 / R^* \langle T \rangle^i \quad (12)$$

where, P_0 is a reference pressure, which is kept constant during the relaxation process, and $R^* = R / M$ and M is the gas molecular mass.

3. NUMERICAL MODEL

The governing equations were discretized using the finite volume procedure Patankar (1980) with a boundary-fitted non-orthogonal coordinate system. The SIMPLE algorithm for the pressure-velocity coupling was adopted to correct both the pressure and the velocity fields. The process starts with the solution of the two momentum equations. Then the velocity field is adjusted in order to satisfy the continuity principle. This adjustment is obtained by solving the pressure correction equation. A computational grid of 266x14 nodes is used in x- and y-direction.

4. RESULTS AND DISCUSSION

4.1 Geometry and coordinate system

Figure 1 presents the geometry of the porous media burner consisting of two distinct regions with different porosities and permeability. The gas mixture enters at the inflow boundary at the left, and the combustion products leave the burner at the outflow boundary at the right. The walls are impermeable and isolated. The porosity ϕ_1 is smaller than ϕ_2 . All numerical parameters are found in Table 1, the activation energy and the pre-exponential factor were obtained from Mohamad et al. (1994).

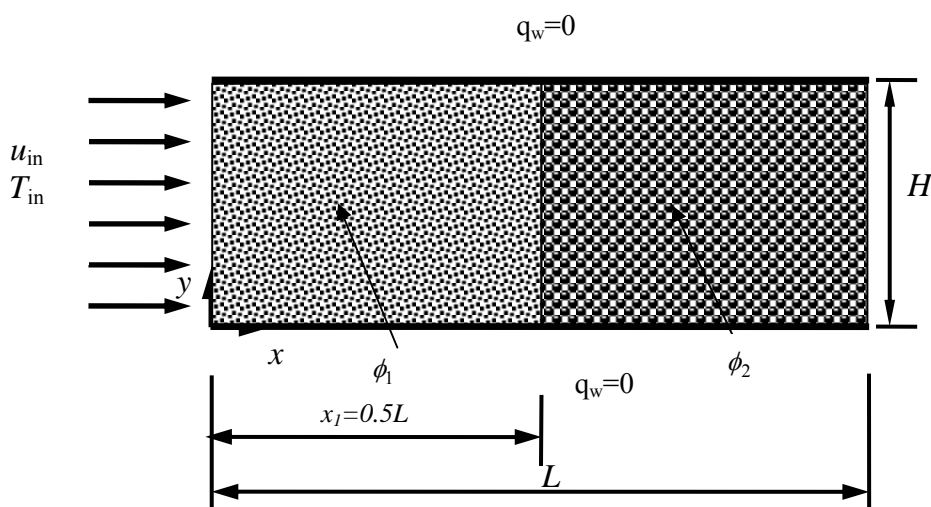


Figure 1. Geometry of a porous inert media burner and coordinate system.

4.2 Boundary conditions

The following boundary conditions are imposed on the solution:

$$\text{at } x=0, u = u_{in}, v=0, \langle T \rangle^i = T_{in}, \langle m_{fu} \rangle^i = m_{fu,in}, \quad (13)$$

$$\text{at } x=L, \frac{\partial \langle T \rangle^i}{\partial x} = \frac{\partial \langle m_{fu} \rangle^i}{\partial x} = \frac{\partial u}{\partial x} = \frac{\partial v}{\partial x} = 0 \quad (14)$$

where, u and v are the components of Darcy velocity vector in x and y . The non-slip condition for velocity is applied on both walls.

4.3 Temperature, concentration, and volumetric rate of fuel consumption profiles

Figure 2 presents the temperature, mass fraction of fuel, volumetric rate of fuel consumption profiles and a comparison with an experiment obtained by Pereira (2002) for a two-dimensional axisymmetric geometry with an inlet velocity of 0.40 m/s, an excess air ratio of 0.67, and an inlet temperature of 335 K. The values for the one dimensional plots were taken at the center line of the combustor.

The profiles indicate that the effect of the porous matrix on the flame structure is the increase of the flame thickness due to the high conductivity of the solid phase.

Table 1. Operating Conditions

Quantity	Value
Activation energy (J/mol) - Ea	130x10 ³
Pre-exponential factor in reaction rate – A (m ³ /kg.s)	3.0x10 ⁸
Length of the combustor – L (cm)	8
H (cm)	4
R (kJ/kmol.K)	8.3145
R* (kJ/kgK)	0.301
P0 (kN/m ²)	101.325
m _{fuel,in}	0.033784
T _{in} (K)	335
Matrix 1:	
K1 (m ²)	0.1477E-07
ϕ_1	0,86
Matrix 2:	
K2 (m ²)	0.3698E-06
ϕ_2	0,90

Figure 3 presents the pressure drop at the center line of the combustor where,

$$PN = \frac{P - P_{MIN}}{P_{MAX} - P_{MIN}} \quad (15)$$

The inflexion point at the abscissa $x/L=0,5$ represents the interface between the two porous materials. It was observed with additional simulations that the combustion affect the pressure drop slightly when compared with the flow without combustion.

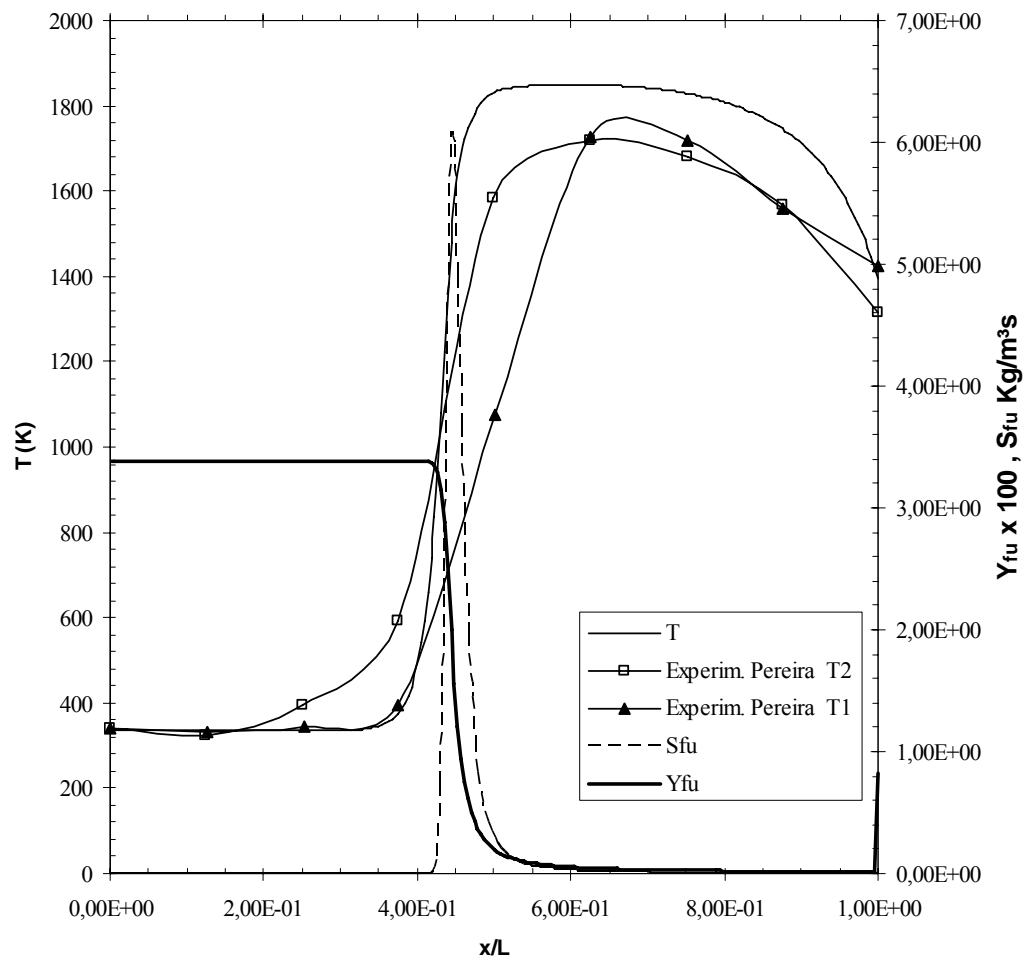


Figure 2. Axial temperature, mass fraction of fuel, volumetric rate of fuel consumption profiles, and a comparison with temperature fields obtained experimentally by Pereira (2002), $y/H=0.5$, $\Psi=0.67$, $u_{in}=0.4$ m/s.

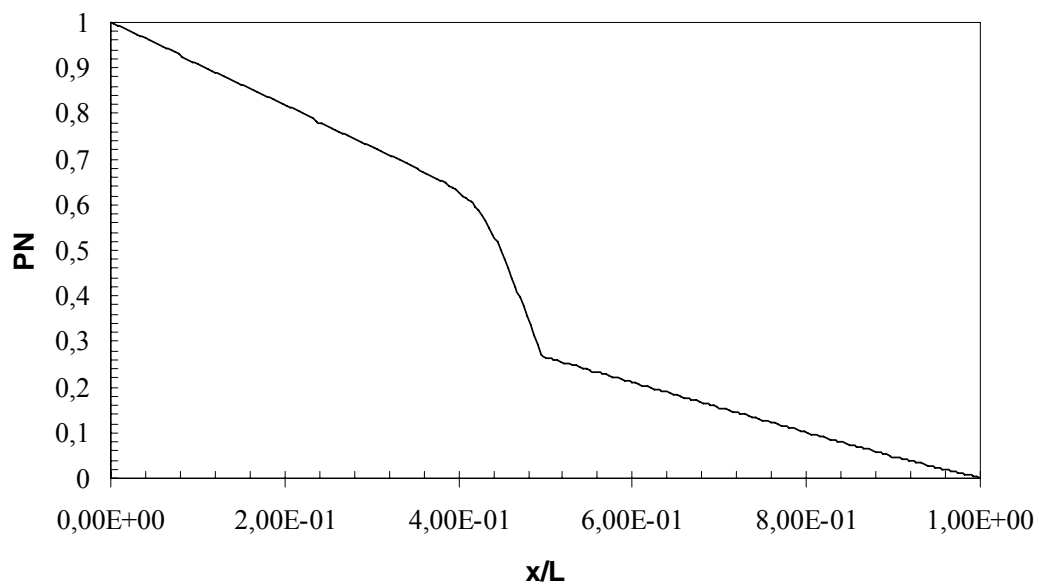


Figure 3. Pressure drop at the center line of the combustor, $u_{in}=0.4$ m/s.

4.4 Effect of inlet velocity on Temperature Profile

Figure 4 presents the effect of increase of inlet velocity on temperature profile for a rectangular adiabatic burner with an excess air ratio of 0.67. The figure indicates that, for laminar flows, the flame moves downstream and stabilizes.

Note that decreasing the inlet velocity decreases the temperature, increasing the excess air ratio decreases the temperature also.

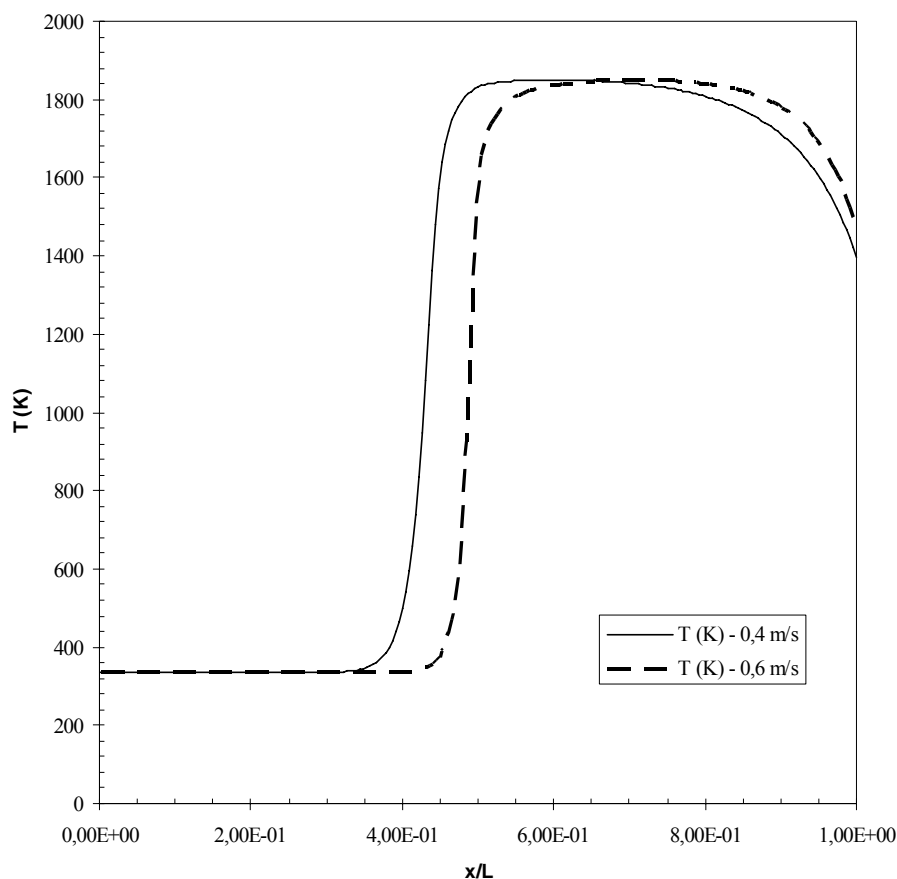


Figure 4. Temperature profiles for different inlet velocities, $\Psi=0.67$.

4.5 Effect of the radiation

In an optically dense medium the diffusion approximation can be applied, the effect of Rosseland mean attenuation coefficient of the matrix 1 is presented in figure 5. In the radiative diffusion approximation the radiation is computed like an increase in the effective conductivity. For a combustion occurring inside a ceramic, with a small solid conductivity like Zirconium Oxide plus Aluminum Oxide, with a porosity of 0.86, an extinction coefficient around 500 (1/m), and $\Psi=0.67$, the conductivity due to radiation can represent more than 80% of the total conductivity. Hence, radiation within the porous media cannot be neglected.

In figure 5 the flame stabilize close to the center of the reactor to an extinction coefficient of 2000 and 3000 (1/m), but, to a smaller value like 1000 the characteristic time of conduction in the matrix 1 is very short making that the flame stabilize close to the entrance of the reactor.

The lost of heat at the outlet due to the radiation decreases the field of temperature close to the outlet of the reactor.

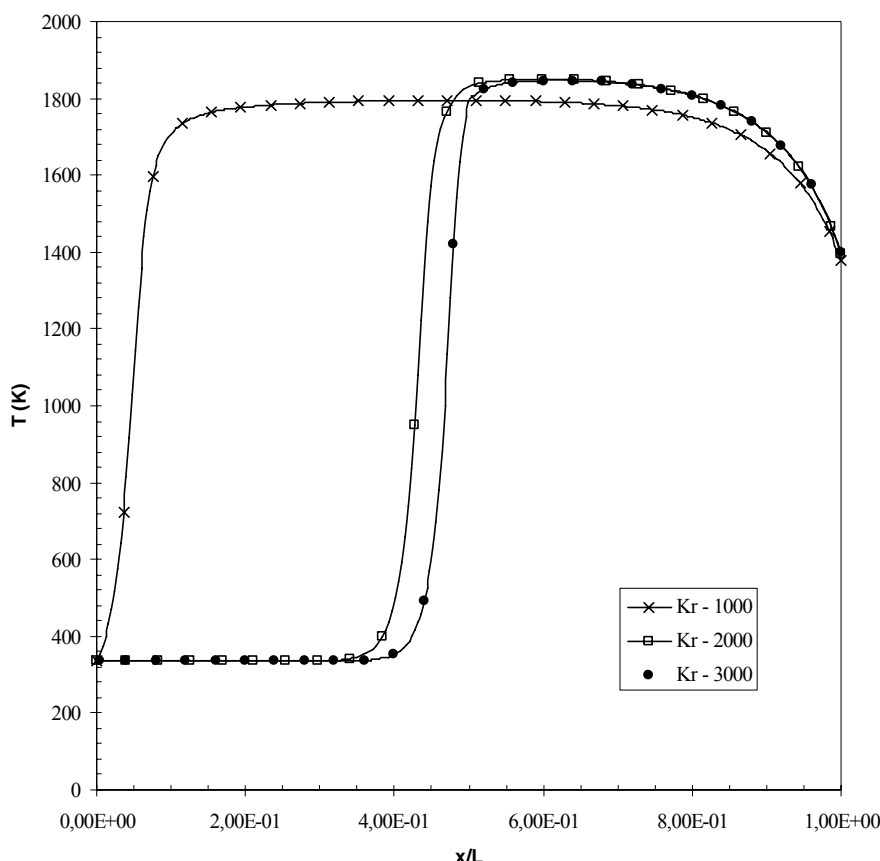


Figure 5. Effect of the Rosseland mean attenuation coefficient at the matrix 1.

5. CONCLUSION

A mathematical model has been developed, and numerically obtained results compared with available experimental data for a porous burner. Temperature and concentration of fuel profiles, flame location, pressure drop, and the effect of radiation have been predicted. Numerical results compare reasonably well with the experimental data.

The model can be used to predict the fields of temperature, mass fraction of the fuel, pressure drop, velocity and the effect of the increase of the power in a two dimensional steady-state combustion problem within porous inert media, better the precision of the values of the physical properties, better results will be obtained. Further work will be carried out in order to simulate pollutants formation in a porous burner.

6. ACKNOWLEDGEMENTS

The authors are thankful to CNPQ, Brazil, for their financial support during the preparation of this work.

7. REFERENCES

- Baek, S. W., 1989, "The Premixed Flame in a Radiatively Active Porous Medium," *Combust. Sci. Technol.*, 64, pp. 277–287.
- Howell, J. R., Hall, M. J., and Ellzey, J. L., 1996, "Combustion of Hydrocarbon Fuels Within Porous Inert Media," *Prog. Energy Combust. Sci.*, 22, pp. 121–145.
- Hsu, P.-F., Howell, J. R., and Matthews, R. D., 1993, "A Numerical Investigation of Premixed Combustion Within Porous Inert Media," *ASME J. of Heat Transfer*, 115, pp. 744–750.
- Jones, W.P., Launder, B.E., 1972, The Prediction of Laminarization with Two-Equation Model of Turbulence , *Int. J. Heat & Mass Transfer*, vol. 15, pp. 301 – 314,
- Kaviany. M.. 1995. *Principles of Heat Transfer in Porous Media*. 2nd edn. Springer. New York.

- Mohamad, A.A., Ramadhyani, S., Viskanta, R, 1994. Modeling of Combustion and Heat-Transfer in a Pcked-Bed with Embedded Coolant Tubes, *Int. J Heat and Mass Transfer*. vol. 37. (8) pp.1181-1191.
- Neef, M., Knaber, P., Summ, G., 1999, Numerical Bifurcation Analysis of Premixed Combustion in Porous Inert Media, unpublished, <http://citeseer.csail.mit.edu/197085.html>
- Pantangi, V. K. and S.C. Mishra, Combustion of gaseous hydrocarbon fuels within porous media – National Conference on Advances in Energy Research, 4-5 December 2006, IIT Bombay.
- Patankar, S. V.. 1980. Numerical Heat Transfer and Fluid Flow. Hemisphere. New York.
- Pereira, F.M., 2002, Medição de características térmicas e estudo do mecanismo de estabilização de chama em queimadores porosos radiantes. Tese de Mestrado, Universidade Federal de Santa Catarina, Brasil.
- Sahraoui, M., Kaviany, 1995, Direct simulation vs Time-Averaged Treatment of Adiabatic, Premixed Flame in a Porous Medium, *Int. J. Heat Mass Transfer*, v.18, pp. 2817-2834.
- Trimis, D., and, Durst, F., 1996, Combustion in a Porous Medium Advances and Applications, *Combust. Sci. Technol*, Vol. 121, pp. 153-168.
- Yoshizawa, Y., Sasaki, K., and Echigo, R., 1988, "Analytical Study of the Structure of Radiation Controlled Flame," *Int. J. Heat Mass Transf.*, 31, pp. 311–319. [Inspec] [ISI]